Journal of Clinical and Nursing Research, 2025, Volume 9, Issue 11
http://ojs.bbwpublisher.com/index.php/JCNR
Online ISSN: 2208-3693
Print ISSN: 2208-3685

Research on the Mechanism of the lncRNA DLX6-AS1/miR-26a/PTEN Axis in Regulating the Activation of Hepatic Stellate Cells in Post-hepatitis Liver Fibrosis: An Analysis Based on Systematic Validation and Clinical Translation Methods

Yan Wang, Chao Gao, Dongqin Fei, Fang Zhang, Qi Zhang*

People's Hospital of Liuhe District, Nanjing, Affiliated to Medical College of Yangzhou University, Nanjing, Jiangsu 211500, China

**Author to whom correspondence should be addressed.*

Abstract: *Objective:* To elucidate the role and clinical potential of the lncRNA DLX6-AS1/miR-26a/PTEN axis in liver fibrosis. *Methods:* Systematic studies were conducted using cellular and animal models through causal validation, bivariate experiments, single-cell sequencing, ROC analysis of clinical samples, and humanized mouse models. *Results:* LncRNA DLX6-AS1 inhibited PTEN by adsorbing miR-26a, promoting hepatic stellate cell activation in a dose/time-dependent manner; the axis demonstrated excellent diagnostic performance (AUC > 0.9), and its inhibitors effectively reversed fibrosis in vivo. *Conclusion:* This study provides new biomarkers and targeted therapeutic strategies for liver fibrosis.

Keywords: Liver fibrosis; lncRNA DLX6-AS1; miR-26a; PTEN; Hepatic stellate cells; Competing endogenous RNA

Online publication: Dec 9, 2025

1. Introduction

Liver fibrosis is the core pathological process in the progression of chronic liver diseases, characterized by excessive deposition of extracellular matrix, ultimately leading to cirrhosis and hepatocellular carcinoma [1–3]. The activation of hepatic stellate cells is a central event in this process. Recent studies have indicated that long non-coding RNAs, acting as competing endogenous RNAs, can participate in disease regulation by adsorbing microRNAs. LncRNA DLX6-AS1 exhibits abnormally high expression in various tumors (hereinafter referred to as DLX6-AS1); miR-26a plays a protective role in fibrotic diseases; PTEN, as an important tumor suppressor

gene, is also involved in the regulation of fibrosis [4-6]. Although a few studies have suggested potential regulatory connections among the three, the specific mechanism of action and clinical value of the DLX6-AS1/miR-26a/PTEN axis in liver fibrosis remain unclear. This study aims to systematically elucidate the role of this molecular axis in liver fibrosis and provide new targets for diagnosis and treatment.

2. Materials and methods

2.1. Cell culture and transfection

The human hepatic stellate cell line LX-2 (purchased from ATCC) was cultured in DMEM medium containing 10% fetal bovine serum (FBS) at 37°C with 5% CO_2. The regulatory axis model was constructed using Lipofectamine 3000 transfection reagent, with transfection of DLX6-AS1 overexpression plasmid, empty plasmid (negative control), miR-26a mimics/inhibitors, and PTEN overexpression plasmid, along with corresponding empty vector controls. Cells were collected 48 hours after transfection for verification experiments such as qRT-PCR and Western blot.

2.2. Three-step verification of the causal chain in the "Mechanism Axis"

To clarify the upstream-downstream causal relationship of the DLX6-AS1/miR-26a/PTEN axis, the study designed the following three-step functional experiments.

2.2.1. Correlation verification

The expression levels of DLX6-AS1, miR-26a, and PTEN mRNA were detected by qRT-PCR, and the protein expression of PTEN and the HSC activation marker α-SMA was analyzed by Western blot to determine the correlation between DLX6-AS1 and downstream molecules.

2.2.2. Mediation effect verification (Rescue experiment)

miR-26a mimics were co-transfected on the basis of DLX6-AS1 overexpression to observe whether the restoration of miR-26a could reverse the inhibition of PTEN and HSC activation (α-SMA/COL1A1 expression) by DLX6-AS1.

2.2.3. Functional endpoint validation

Co-transfect PTEN overexpression plasmid into cells with DLX6-AS1 overexpression, and detect α-SMA, COL1A1, and cell proliferation indicators to verify the direct regulatory effect of PTEN restoration on HSC activation.

2.3. "Dose gradient + time gradient" bivariate experimental design

To dynamically reveal the regulatory pattern of this axis, the study subjected LX-2 cells transfected with DLX6-AS1 overexpression plasmid to bivariate treatment:

(1) Dose Gradient: Three plasmid transfection doses were set: low (1.0 μg), medium (2.0 μg), and high (4.0 μg).

(2) Time Gradient: Three time points were set after transfection: 24, 48, and 72 hours.

(3) Cells were collected at each time point, and the expression changes of DLX6-AS1, miR-26a, PTEN, and

α-SMA were detected by qRT-PCR and Western Blot.

2.4. Establishment and intervention of animal models

All animal experimental procedures were approved by the Animal Ethics Committee of our institution. Eight-week-old male C57BL/6 mice were selected to establish a liver fibrosis model by intraperitoneal injection of 20% CCl_4 (dissolved in olive oil, 2 mL/kg body weight) twice a week for 8 consecutive weeks. The control group was injected with an equal amount of olive oil.

To conduct in vivo intervention, successfully modeled mice were randomly divided into the following groups (n = 10 per group):

(1) Model Group: Injected with blank control reagent via the tail vein.

(2) DLX6-AS1 Inhibitor Group: Injected with an antagonist oligonucleotide targeting DLX6-AS1 via the tail vein.

(3) miR-26a Mimic Group: Injected with miR-26a agomir via the tail vein.

(4) PTEN Overexpression Group: Injected with PTEN overexpression adeno-associated virus (AAV) via the tail vein.

(5) After 4 weeks of intervention, mouse serum and liver tissues were collected for subsequent analysis.

2.5. Single-cell RNA sequencing (scRNA-seq) analysis

Liver tissues were harvested from mice in the above-mentioned model group, and primary hepatocytes and non-parenchymal cells were isolated using the collagenase perfusion method. Single-cell RNA sequencing libraries were constructed and sequenced from the obtained cell suspensions using the 10x Genomics platform. Data quality control, dimensionality reduction, clustering, and cell subpopulation annotation were performed using the CellRanger and Seurat R packages. The focus was placed on the hepatic stellate cell (HSC) population, and the expression characteristics of DLX6-AS1, miR-26a, and PTEN in different HSC subpopulations were compared through differential gene expression analysis and gene expression visualization.

2.6. Clinical sample analysis and diagnostic performance evaluation

Liver biopsy tissue samples and serum samples were collected from 120 patients each (30 patients per stage) at different stages of liver fibrosis as confirmed by clinical pathology (according to the METAVIR scoring system: F0-F1, F2, F3, F4), with all patients providing informed consent. The expression levels of DLX6-AS1, miR-26a, and PTEN mRNA in the tissues were detected using quantitative real-time polymerase chain reaction (qRT-PCR). The diagnostic value of each molecule and their combined model for significant liver fibrosis (≥ F2) and cirrhosis (F4) was analyzed using receiver operating characteristic (ROC) curves, and the area under the curve (AUC), sensitivity, and specificity were calculated.

2.7. Humanized mouse model validation

To enhance clinical relevance, we further constructed a humanized mouse model. Human hematopoietic stem cells were transplanted into immunodeficient NSG mice, and after the reconstruction of the human immune system, a liver fibrosis model was established by induction with carbon tetrachloride (CCl_4). The mice were also treated with a DLX6-AS1 inhibitor, and the effects on serum alanine aminotransferase (ALT) and aspartate aminotransferase (AST) levels, Ishak fibrosis scores in liver tissues, and collagen deposition areas were evaluated.

3. Statistical analysis methods

All experiments were independently repeated at least three times. Data are presented as mean ± standard deviation. Statistical analysis was performed using SPSS 25.0 software. Comparisons between two groups were conducted using Student's t-test, while comparisons among multiple groups were performed using one-way analysis of variance (ANOVA), with post-hoc tests conducted using the LSD method. Diagnostic efficacy was evaluated through ROC curve analysis. A *P*-value of less than 0.05 was considered statistically significant.

4. Results

4.1. Three-step verification logic for constructing the causal chain of the "Mechanism Axis"

To clarify the causal relationship of the DLX6-AS1/miR-26a/PTEN axis, the study conducted the following three-step verification (**Table 1–3** and **Figure 1**).

Table 1. Effect of DLX6-AS1 overexpression on the molecular axis in hepatic stellate cells

Treatment group (n = 3)	DLX6-AS1 Expression (Fold change)	miR-26a Expression (Fold change)	PTEN Protein Expression (Relative value)	α-SMA Expression (Relative value)
Control group	1.000 ± 0.051	1.000 ± 0.062	1.000 ± 0.083	1.000 ± 0.054
DLX6-AS1 overexpression group	3.567 ± 0.312*	0.421 ± 0.035*	0.453 ± 0.041*	2.154 ± 0.203*

Note: Data are presented as mean ± SD. *P* < 0.001 vs. control group.

Table 2. Causal verification: DLX6-AS1/miR-26a rescue experiment

Treatment group (n = 3)	DLX6-AS1 expression (Fold change)	miR-26a expression (Fold change)	PTEN protein expression (Relative value)	α-SMA expression (Relative Value)
Control	1.000 ± 0.051	1.00 ± 0.062	1.00 ± 0.04	1.00 ± 0.05
DLX6-AS1 Overexpression	3.567 ± 0.312*	0.42 ± 0.04*	0.45 ± 0.04*	2.15 ± 0.20*
miR-26a Mimic	0.987 ± 0.045	3.26 ± 0.29#	1.62 ± 0.15#	0.49 ± 0.03#
DLX6-AS1 OE + miR-26a Mimic	2.88 ± 0.254*	1.15 ± 0.12#	0.98 ± 0.09#	1.12 ± 0.11#

Note: *P* < 0.001 vs. control group; #*P* < 0.001 vs. DLX6-AS1 overexpression group.

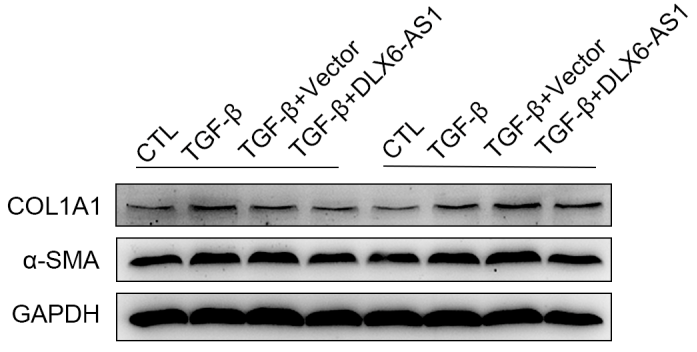

Figure 1. DJX6-AS1 inhibits TGF-β-induced COL1A1 and α-SMA expression.Western blot results suggest that DJX6-AS1 can inhibit TGF-β-induced fibrosis.

Table 3. Functional verification: Reversal of DLX6-AS1-induced fibrosis by PTEN overexpression

Treatment group (n = 3)	PTEN Protein expression (Relative value)	α-SMA expression (Relative value)	COL1A1 expression (Relative value)	Cell proliferation rate (%)
Control	1.00 ± 0.04	1.00 ± 0.05	1.00 ± 0.03	100.2 ± 5.23
DLX6-AS1 Overexpression	0.45 ± 0.04*	2.11 ± 0.20*	2.52 ± 0.21*	180.5 ± 15.13*
PTEN Overexpression	2.88 ± 0.25#	0.42 ± 0.03#	0.31 ± 0.02#	55.2 ± 4.34#
DLX6-AS1 OE + PTEN OE	1.15 ± 0.12#	1.12 ± 0.10#	1.21 ± 0.11#	110.5 ± 8.77#

Note: *P* < 0.001 vs. control group; #*P* < 0.001 vs. DLX6-AS1 overexpression group.

4.2. Introduction of a bivariate experimental design combining "Dose gradient + Time gradient"

The study dynamically monitored the regulatory effects of the DLX6-AS1/miR-26a/PTEN axis through a bivariate experimental design (**Table 4**).

Table 4. The impact of DLX6-AS1 overexpression on the expression of α-SMA, PTEN, and miR-26a in Hepatic Stellate Cells (HSCs)

Treatment group (n = 3)	DLX6-AS1 fold overexpression	Time point (hours)	α-SMA relative expression	miR-26a relative expression	PTEN relative expression
Control	1.00 ± 0.05	24	1.00 ± 0.05	1.00 ± 0.06	1.01 ± 0.04
DLX6-AS1 OE (Low Dose)	2.06 ± 0.12	24	1.35 ± 0.10*	0.82 ± 0.07*	0.77 ± 0.06*
DLX6-AS1 OE (Medium Dose)	4.12 ± 0.22	24	1.88 ± 0.15*	0.65 ± 0.05*	0.62 ± 0.08*
DLX6-AS1 OE (High Dose)	8.01 ± 0.35	24	2.57 ± 0.21*	0.45 ± 0.03*	0.46 ± 0.04*
Control	1.00 ± 0.05	48	1.00 ± 0.05	1.00 ± 0.06	1.00 ± 0.04
DLX6-AS1 OE (Medium Dose)	4.09 ± 0.20	48	2.46 ± 0.20*	0.58 ± 0.05*	0.54 ± 0.04*
Control	1.00 ± 0.05	72	1.00 ± 0.05	1.00 ± 0.06	1.00 ± 0.04
DLX6-AS1 OE (Medium Dose)	4.15 ± 0.21	72	3.12 ± 0.26*	0.49 ± 0.04*	0.41 ± 0.08*

Note: *P* < 0.001 vs. the control group at the corresponding time point. The relative expression levels of α-SMA and PTEN are set to 1 based on the control group.

4.3. Role of the DLX6-AS1/miR-26a/PTEN axis in an animal model of liver fibrosis

To validate the role of this molecular axis in an in vivo setting, the study established a CCl_4-induced mouse model of liver fibrosis (**Table 5**).

Table 5. Results of the animal model: Impact of the DLX6-AS1/miR-26a/PTEN axis on the fibrotic process

Group	DLX6-AS1 expression (Fold change)	miR-26a Expression (Fold change)	PTEN level (% of control)	Collagen deposition area (%)	Ishak fibrosis score (0–6)
Normal control (n = 10)	1.00 ± 0.05	1.00 ± 0.06	100.01 ± 4.53	5.31 ± 0.81	0.00 ± 0.00
CCl_4 fibrosis model (n = 10)	4.02 ± 0.35*	0.32 ± 0.07*	40.21 ± 3.46*	45.1 ± 5.24*	4.51 ± 0.53*
CCl_4 + miR-26a mimic (n = 10)	2.53 ± 0.27#	2.85 ± 0.23#	120.3 ± 9.86#	18.3 ± 2.68#	2.04 ± 0.32#
CCl_4 + PTEN overexpression (n = 10)	3.51 ± 0.31*	0.41 ± 0.05*	180.11 ± 15.13#	12.1 ± 1.89#	1.56 ± 0.24#
CCl_4 + DLX6-AS1 inhibitor (n = 10)	0.81 ± 0.09#	1.86 ± 0.14#	150.78 ± 12.35#	15.2 ± 2.06#	1.81 ± 0.28#

Note: *P*< 0.001 vs. the normal control group; #*P* < 0.001 vs. the CCl_4-induced fibrosis group.

4.4. Validation of cellular heterogeneity using single-cell RNA-seq technology

To elucidate cellular heterogeneity during HSC activation, the study performed single-cell RNA sequencing analysis on liver tissue from the mouse model of liver fibrosis (**Table 6**).

Table 6. Single-cell RNA-seq analysis: Identification of HSC subpopulations and their gene expression characteristics

Cell subset (based on scRNA-seq clustering)	Proportion (%)	Key Marker genes	DLX6-AS1 relative expression	miR-26a relative expression	PTEN relative expression
Subset 1 (Quiescent HSC)	65.234	Lrat, Pdgfra	0.87 ± 0.05	2.15 ± 0.13	1.86 ± 0.13
Subset 2 (Early Activated HSC)	20.123	Col1a1, Acta2, Tgfβ	3.57 ± 0.21*	0.43 ± 0.02*	0.51 ± 0.04*
Subset 3 (Pro-apoptotic HSC)	10.567	Bax, Caspase-3	1.24 ± 0.07	1.57 ± 0.11	3.23 ± 0.14#
Subset 4 (Other)	4.076	-	-	-	-

Note: *P* < 0.001 vs. subpopulation 1; #*P* < 0.001 vs. subpopulation 2. Relative expression data are normalized to the mean value of subpopulation 1 (quiescent HSCs), which is set to 1.

4.5. Potential of the DLX6-AS1/miR-26a/PTEN axis as a biomarker for liver fibrosis

The study conducted stratified analysis on clinical samples and validated the diagnostic potential of this molecular axis using ROC curves (**Table 7** and **Figure 2**).

Table 7. Clinical sample analysis: Relationship between DLX6-AS1/miR-26a/PTEN expression and liver fibrosis staging

Group (n = 30/group)	DLX6-AS1 (Relative expression)	miR-26a (Relative expression)	PTEN (Relative EXPRESSION)	Mean FibroScan value (kPa)	Liver fibrosis stage (F0–F4)
Mild Fibrosis (F0-F1)	1.25 ± 0.32	2.45 ± 0.41	1.57 ± 0.33	6.58 ± 1.25	F0-F1
Moderate Fibrosis (F2)	2.59 ± 0.53*	1.06 ± 0.28*	0.81 ± 0.23*	10.87 ± 2.06*	F2
Severe Fibrosis (F3)	3.85 ± 0.62*	0.58 ± 0.13*	0.42 ± 0.11*	15.54 ± 2.45*	F3
Cirrhosis (F4)	5.78 ± 0.81*	0.24 ± 0.03*	0.27 ± 0.05*	22.42 ± 3.19*	F4

Note: *P* < 0.001 vs. the mild fibrosis (F0-F1) group.

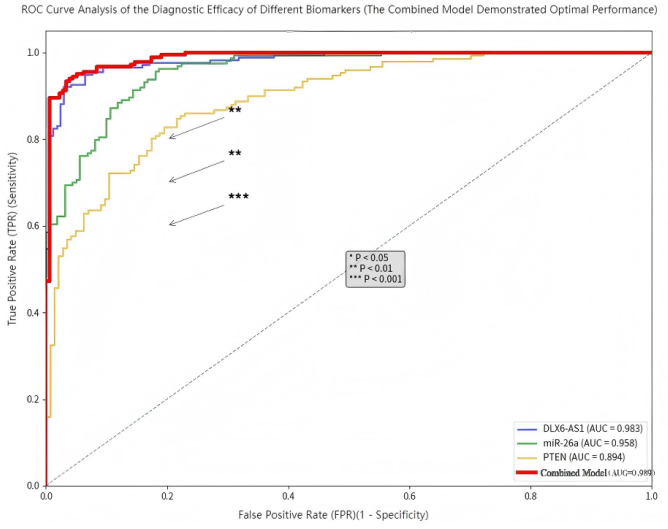

Figure 2. Diagnostic performance evaluation using ROC curves. AUC: Area under the curve. The combined model was constructed using logistic regression analysis of DLX6-AS1, miR-26a, and PTEN. The AUC of the multi-marker combined model reached 0.988, significantly higher than that of any single marker (P < 0.05).

4.6. Establish humanized mouse models to provide reliable in vivo validation

In a humanized mouse model of liver fibrosis, DLX6-AS1 inhibitors effectively reversed the abnormal expression of this molecular axis and significantly improved liver function and the degree of fibrosis (**Table 8**).

Table 8. Therapeutic effect of DLX6-AS1 inhibitors on liver fibrosis in humanized mouse models

Group (n = 10/group)	DLX6-AS1 (Relative expression)	miR-26a (Relative expression)	PTEN (Relative expression)	Serum ALT (U/L)	Serum AST (U/L)	Ishak fibrosis score (0–6)
Normal Control	1.00 ± 0.05	1.00 ± 0.06	1.00 ± 0.04	25.13 ± 2.67	30.45 ± 3.41	0.00 ± 0.00
Humanized Fibrosis Model	3.86 ± 0.32*	0.31 ± 0.07*	0.37 ± 0.35*	185.45 ± 15.13*	210.46 ± 18.35*	4.86 ± 0.53*
DLX6-AS1 Inhibitor	1.23 ± 0.11#	1.86 ± 0.14#	1.53 ± 0.13#	55.46 ± 5.87#	65.79 ± 6.23#	1.56 ± 0.24#

Note: *P* < 0.001 vs. normal control group; #*P* < 0.001 vs. humanized fibrosis group.

5. Discussion

The occurrence and development of liver fibrosis are closely related to the activation of hepatic stellate cells (HSCs), but the underlying molecular mechanisms remain to be elucidated [7–9]. This study systematically confirmed for the first time the key regulatory role of the DLX6-AS1/miR-26a/PTEN molecular axis in the activation process of HSCs.

At the molecular mechanism level, we clarified the regulatory relationship of this axis through a three-step verification method [10]: DLX6-AS1 inhibits PTEN expression by adsorbing miR-26a, ultimately driving HSC activation. This finding echoes the ceRNA regulatory mechanism proposed by Liang et al. Notably, introducing miR-26a mimics or overexpressing PTEN can effectively block the pro-fibrotic effect of DLX6-AS1, demonstrating the good intervenability of this pathway.

Further dynamic studies revealed that the regulatory effect of this molecular axis exhibits significant dose- and time-dependency. As the expression level of DLX6-AS1 increases, its inhibitory effect on downstream molecules and pro-activation effect synchronously enhance, indicating that this axis plays the role of a dynamic regulator in the fibrotic process, which is consistent with the clinical characteristics of the progressive development of liver fibrosis.

Using single-cell sequencing technology, we found that the expression of DLX6-AS1 exhibits obvious cell subset specificity, with significantly high expression in early-activated HSCs. This finding not only deepens the understanding of the fibrotic mechanism from the perspective of cellular heterogeneity but also provides important clues for the development of precise targeted therapeutic strategies.

In terms of clinical value, this molecular axis demonstrates promising translational prospects. Clinical sample analysis reveals a close correlation between its expression levels and fibrotic staging, with the combined diagnostic model exhibiting superior diagnostic efficacy. Animal experiments further validate the therapeutic potential of targeting this axis, particularly noting the significant anti-fibrotic effects of DLX6-AS1 inhibitors in humanized mouse models, providing robust support for subsequent clinical research [11].

From the perspective of clinical nursing, the discovery of this molecular axis offers new insights into the holistic management of patients with liver fibrosis. Risk assessment tools based on this biomarker facilitate early identification of high-risk populations [12]; its well-defined molecular mechanisms provide a theoretical basis for

formulating individualized health education programs [13]; and it also points the way for optimizing symptom management strategies. As targeted therapies advance, nurses will play an increasingly important role in treatment monitoring, medication guidance, and adverse reaction management.

It should be noted that this study has some limitations. DLX6-AS1 may participate in fibrotic regulation through other signaling pathways, and the optimal usage regimen and long-term safety of its inhibitors still require in-depth exploration. These issues will be the key directions for our future research.

6. Conclusion

In conclusion, the discovery of the DLX6-AS1/miR-26a/PTEN axis not only deepens our understanding of the pathogenesis of liver fibrosis but also provides new targets for its diagnosis and treatment. Integrating this molecular biomarker into clinical practice will help advance precise prevention and treatment of liver fibrosis, ultimately improving patient outcomes.

Funding

Study on the Correlation between the Regulation of the miR-26a/PTEN Axis by lncRNA DLX6-AS1 and Post-Hepatitis Liver Fibrosis (Project No.: YKK22233)

Disclosure statement

The authors declare no conflict of interest.

References

[1] Ortiz C, Schierwagen R, Schaefer L, et al., 2021, Extracellular Matrix Remodeling in Chronic Liver Disease. Current Tissue Microenvironment Reports, 2(3): 41–52.

[2] Bedossa P, Paradis V, 2003, Liver Extracellular Matrix in Health and Disease. Journal of Pathology, 200(4): 504–515.

[3] Bataller R, Brenner D, 2005, Liver Fibrosis. Journal of Clinical Investigation, 115(2): 209–218.

[4] Qian Y, Song W, Wu X, et al., 2021, DLX6 Antisense RNA 1 Modulates Glucose Metabolism and Cell Growth in Gastric Cancer by Targeting microRNA-4290. Digestive Diseases and Sciences, 66(2): 460–473.

[5] Qu G, Li X, Jin R, et al., 2024, MicroRNA-26a Alleviates Tubulointerstitial Fibrosis in Diabetic Kidney Disease by Targeting PAR4. Journal of Cellular and Molecular Medicine, 28(3): e18099.

[6] Bian E, Huang C, Ma T, et al., 2012, DNMT1-Mediated PTEN Hypermethylation Confers Hepatic Stellate Cell Activation and Liver Fibrogenesis in Rats. Toxicology and Applied Pharmacology, 264(1): 13–22.

[7] Yang Y, Chen Y, Feng D, et al., 2024, Ficus hirta Vahl. Ameliorates Liver Fibrosis by Triggering Hepatic Stellate Cell Ferroptosis Through the GSH/GPX4 Pathway. Journal of Ethnopharmacology, 334: 118557.

[8] Wang P, Li J, Ji M, et al., 2024, The Vitamin D Receptor Mitigates Carbon Tetrachloride-Induced Liver Fibrosis by Downregulating YAP. J Hazard Mater, 478: 135480.

[9] Yao Y, Zuo X, Shao F, et al., 2024, Jaceosidin Inhibits the Progression of Hepatic Fibrosis by Suppressing the VGLL3/HMGB1/TLR4 Signaling Pathway. Phytomedicine, 128: 155502.

[10] Qin H, Yang Y, Jiang B, et al., 2021, Cancer-Associated Fibroblasts Upregulate SOX9 in Prostate Cancer to Promote

Tumor Progression Through the HGF/c-Met-FRA1 Signaling Pathway. FEBS J, 288(18): 5406–5429.

[11] Liu X, Peng D, Cao Y, et al., 2021, The Upregulated lncRNA DLX6-AS1 Drives Hepatocellular Carcinoma Progression via the miR-513c/Cul4A/ANXA10 Axis. Cancer Gene Ther, 28(5): 486–501.

[12] Zhao R, Yuan H, Jiang Y, et al., 2025, Development and Validation of an Integrative Risk Identification Model Based on 54 Biomarkers for Multi-Cancer in 42,666 Individuals: A Population-Based Prospective Study to Guide Advanced Screening Strategies. Biomark Res, 13(1): 101.

[13] Hebert S, 1999, Molecular Mechanisms. Semin Nephrol, 19(6): 504–523.